Journal of Structural Engineering and Geotechnics,

7 (1), 67 -73, Winter 2017

Implementing Basic Displacement Function to Analyze Free Vibration Rotation of Non-Prismatic Euler-Bernoulli Beams

Pouria Hajikarimi[a] , Reza Attarnejad[*,b]

[a] *Instructor, Department of Civil Engineering, Qazvin Branch, Islamic Azad University, Qazvin, Iran*

[b]*Professor, School of Civil Engineering, College of Engineering, University of Tehran, Tehran, Iran*

Received 2 October 2016, Accepted 18 December 2016

Abstract

Rotating beams have been considerably appealing to engineers and designers of complex structures i.e. aircraft's propeller and windmill turbines. In this paper, a new flexibility-based method is proposed for the dynamic analysis of rotating non-prismatic Euler-Bernoulli beams. The flexibility basis of the method ensures the true satisfaction of equilibrium equations at any interior point of the elements. Following structural/mechanical principles, exact shape functions and consequently exact structural matrices i.e. consistent mass, geometric stiffness and flexural stiffness matrices are derived in terms of special so-called "Basic Displacement Functions". The method is considered as the logical extension of conventional finite element method. Being straightforward formulated, the method can be incorporated into any standard finite element programs. The method poses no restrictions on either type of cross-section or variation of cross-sectional dimensions. The effects of rotational speed parameter and taper ratio on the variation of natural frequencies are studied and the results compare well with the other existing methods in the technical literature.

Keywords: *Free vibration; Non-prismatic; Euler-Bernoulli beam; Basic Displacement Functions; Energy methods*

1. Introduction

Free vibration analysis of non-rotating tapered Euler-Bernoulli beams have has been investigated by many researches researchers [1-4]. The free analysis of rotating tapered beams have received great attention from designers of rotating machineries such as windmills, aircraft propellers due to its significant effect on their performance especially in presence of time-dependent loads. Obtaining natural frequencies of the system as an important component of free vibration analysis provides worthy insight for the designers in order to understand the response of the structural systems to dynamic loads.The presence of variable coefficients in the governing differential equation of motion introduced by varying cross-sectional area, moment of inertia and centrifugal forces is the troublesome point in the analysis of rotating tapered beams; hence it seems that derivation of a closed-form solution is impossible. Through years, many approximatenumerical techniques have been proposed such as dynamic stiffness method [5-7], finite element method [8-9] and series solution of governing equation of motion [10, 11]. Understanding the fact that Hermite shape functions do not satisfy the homogeneous part of the static governing equation, Gunda and Ganguli [12] proposed new rational shape functions which satisfy the homogeneous static part. They [12] verified their method for both static and free vibration analyses of tapered beams. Using Frobenius method, Banerjee et al. [7] derived the dynamic stiffness matrix for non-prismatic beams whose cross-sectional area and moment of inertia vary respectively along beam length with arbitrary integer powers n and n+2. Considering the similar assumptions for cross-sectional area and moment of inertia as in Ref. [7], Ozgumus and Kaya [13] carried out free vibration analysis for tapered rotating beams using differential transform method (DTM). Mei [14] determined natural frequencies of rotating prismatic beam via application of DTM to the governing equation of motion.

In this paper, new set of functions namely Basic Displacement Functions (BDFs) are introduced

*Corresponding Author Email address: attarnejad@ut.ac.ir

which hold mechanical interpretations. Considering basic structural/mechanical theorems, it is shown that exact shape functions are expressed in terms of BDFs; thus exact structural matrices are evaluated. The effects of centrifugal forces are introduced into the formulation by adding the geometric stiffness matrix to the flexural one. This method has been previously employed for the analysis of non-rotating tapered members by the first author [15-16]. The method is considered as the logical extension of the conventional finite elements method and can be easily incorporated into the existing finite element programs.

2. Basic Displacement Functions

In the following, four BDFs are introduced as,

b_{v1}: Transverse displacement of the left node due to a unit load at distance $\bar{x}$ when the beam is clamped at right as shown in Figure (1-a).

$b_{\theta 1}$: Bending rotation angle of the left node due to a unit load at distance $\bar{x}$ when the beam is clamped at right as shown in Figure (1-b).

b_{v2}: Transverse displacement of the right node due to a unit load at distance $\bar{x}$ when the beam is clamped at left as shown in Figure (1-c).

$b_{\theta 2}$: Bending rotation angle of the right node due to a unit load at distance $\bar{x}$ when the beam is clamped at left as shown in Figure (1-d).

Due to the structural definitions of BDFs, it is easily verified that each BDFs could be given via application of basic structural theorems such as the energy methods [17].

$$b_{v1}(\bar{x}) = \int_{\bar{x}}^{l} \frac{s(s-\bar{x})}{EI(s)} ds \tag{1}$$

$$b_{\theta 1}(\bar{x}) = \int_{\bar{x}}^{l} \frac{-(s-\bar{x})}{EI(s)} \tag{2}$$

$$b_{v2}(\bar{x}) = \int_{0}^{\bar{x}} \frac{(l-s)(\bar{x}-s)}{EI(s)} \tag{3}$$

$$b_{\theta 2}(\bar{x}) = \int_{0}^{\bar{x}} \frac{-(s-\bar{x})}{EI(s)} ds \tag{4}$$

where l and EI are length of the element and the flexural rigidity, respectively. On the basis of the reciprocal theorem [17], BDFs can equivalently be interpreted mechanically as,

b_{v1}: Transverse displacement at distance $\bar{x}$ due to a unit load at the left node of a beam clamped at right as shown in Figure (2-a).

$b_{\theta 1}$: Angle of rotation at distance $\bar{x}$ due to a unit moment at the left node of a beam clamped at right as shown in Figure (2-b).

b_{v2}: Transverse displacement at distance $\bar{x}$ due to a unit load at the right node of a beam clamped at left as shown in Figure (2-c).

$b_{\theta 2}$: Angle of rotation at distance $\bar{x}$ due to a unit moment at the right node of a beam clamped at left as shown in Figure (2-d).

Considering the equivalent definitions of BDFs, it is observed that both the first and second derivatives of BDFs have mechanical interpretations, as well, where they are respectively defined as the slope and curvature of the corresponding beam. The derivatives of BDFs are given in Table 1.

$$F_{11} = \begin{bmatrix} b_{v1}(0) & b_{\theta 1}(0) \\ \left.\frac{db_{v1}}{d\bar{x}}\right|_{\bar{x}=0} & \left.\frac{db_{\theta 1}}{d\bar{x}}\right|_{\bar{x}=0} \end{bmatrix} \tag{5}$$

$$F_{22} = \begin{bmatrix} b_{v2}(l) & b_{\theta 2}(l) \\ \left.\frac{db_{v2}}{d\bar{x}}\right|_{\bar{x}=l} & \left.\frac{db_{\theta 2}}{d\bar{x}}\right|_{\bar{x}=l} \end{bmatrix} \tag{6}$$

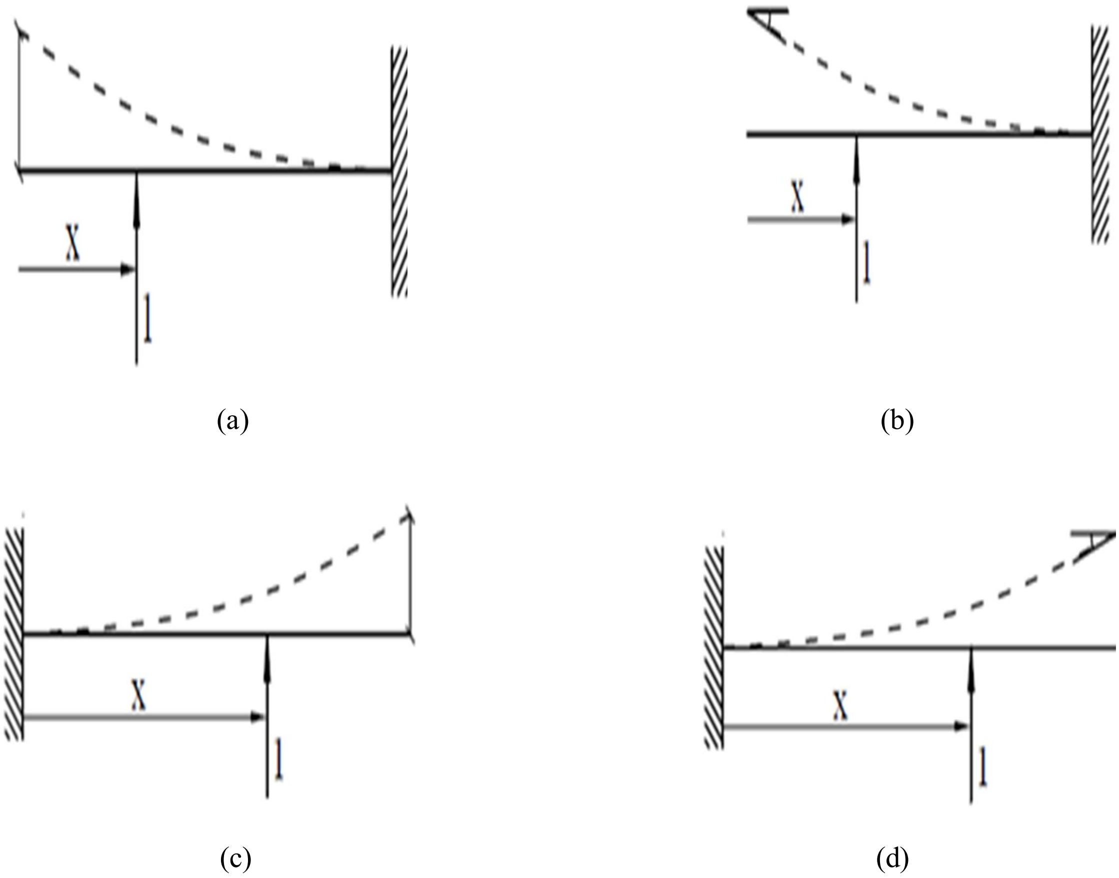

Figure 1.Mechanical illustrations of BDFs

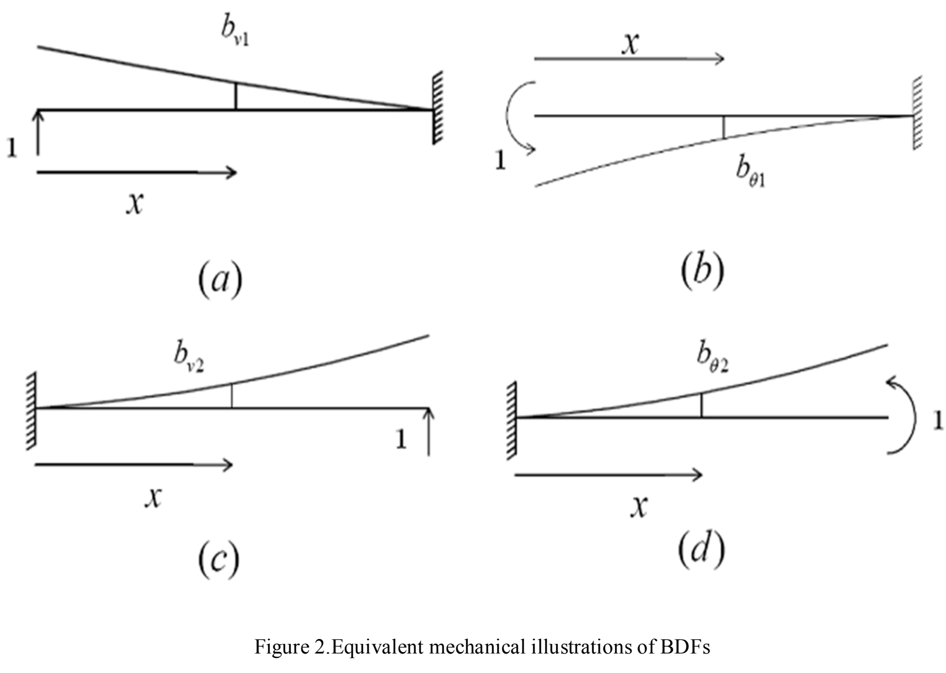

Figure 2.Equivalent mechanical illustrations of BDFs

Table 1.First and second derivatives of BDFs

Type of BDF	First Derivative	Second Derivative
b_{v1}	$\int_{\bar{x}}^{l} \frac{-s}{EI(s)} ds$	$\frac{\bar{x}}{EI(\bar{x})}$
$b_{\theta 1}$	$\int_{\bar{x}}^{l} \frac{1}{EI(s)} ds$	$\frac{-1}{EI(\bar{x})}$
b_{v2}	$\int_{0}^{\bar{x}} \frac{l-s}{EI(s)} ds$	$\frac{l-\bar{x}}{EI(\bar{x})}$
$b_{\theta 2}$	$\int_{0}^{\bar{x}} \frac{1}{EI(s)} ds$	$\frac{1}{EI(\bar{x})}$

In which $\mathbf{F}_{11}, \mathbf{F}_{22}$ are nodal flexibility matrices of the first and second node, respectively.

3. Application of BDFs

Assume a general beam shown in Figure 3. In order to obtain the nodal reactions, the original structural system is decomposed into isostatic structures i.e. cantilever beams and the boundary conditions are imposed for the released support.
Scrutinizing the definitions of equivalent BDFs, one can easily evaluate the nodal flexibility matrices as
The nodal displacements of point (2) in Figure (3-b) can be elegantly computed in terms of BDFs as,

$$\begin{Bmatrix} w_2 \\ \theta_2 \end{Bmatrix}^{(b)} = \int_0^l q(\bar{x}) \begin{Bmatrix} b_{v2} \\ b_{\theta 2} \end{Bmatrix} d\bar{x} \tag{7}$$

In which $q(\bar{x})$ is the external distributed transverse loading. Apparently the nodal displacements of point (2) in Figure (3-c) are given as,

$$\begin{Bmatrix} w_2 \\ \theta_2 \end{Bmatrix}^{(c)} = \mathbf{F}_{22} \begin{Bmatrix} V_2 \\ M_2 \end{Bmatrix} \tag{8}$$

Imposing the boundary conditions at point (2)

$$\begin{Bmatrix} w_2 \\ \theta_2 \end{Bmatrix} = \begin{Bmatrix} w_2 \\ \theta_2 \end{Bmatrix}^{(b)} + \begin{Bmatrix} w_2 \\ \theta_2 \end{Bmatrix}^{(c)} = 0 \tag{9}$$

The nodal reactions are obtained by substituting Eqs. (7, 8) in Eq. (9)

$$\begin{Bmatrix} V_2 \\ M_2 \end{Bmatrix} = -\mathbf{K}_{22} \int_0^l q(\bar{x}) \begin{Bmatrix} b_{v2} \\ b_{\theta 2} \end{Bmatrix} d\bar{x} \tag{10}$$

Similarly the nodal reactions of point (1) are obtained.

$$\begin{Bmatrix} V_1 \\ M_1 \end{Bmatrix} = -\mathbf{K}_{11} \int_0^l q(\bar{x}) \begin{Bmatrix} b_{v1} \\ b_{\theta 1} \end{Bmatrix} d\bar{x} \tag{11}$$

Based on structural analysis, nodal equivalent forces are the negative of nodal reactions; thus

$$\mathbf{F} = \mathbf{G} \int_0^l q(\bar{x}) \mathbf{b} d\bar{x} \tag{12}$$

in which

$$\mathbf{G} = \begin{bmatrix} \mathbf{K}_{11} & 0 \\ 0 & \mathbf{K}_{22} \end{bmatrix} \tag{13}$$

$$\mathbf{b} = \{ b_{v1} \quad b_{\theta 1} \quad b_{v2} \quad b_{\theta 2} \}^T \tag{14}$$

$$\mathbf{F}=\{V_1 \ \ M_1 \ \ V_2 \ \ M_2\}^T \tag{15}$$

Comparing Eq. (12) with the relation proposed by finite element method

$$\mathbf{F} = \int_0^l q(\bar{x}).\mathbf{N}.d\bar{x} \tag{16}$$

The shape functions $\mathbf{N}$ are obtained as,

$$\mathbf{N} = \mathbf{b}^T.\mathbf{G} \tag{17}$$

Once shape functions are derived, the structural matrices can be evaluated as [1],

$$\mathbf{M} = \int_0^l \mathbf{N}^\mathbf{T}.\rho A(\bar{x}).\mathbf{N}.d\bar{x} \tag{18}$$

$$\mathbf{K_G} = \int_0^l \mathbf{N}'^\mathbf{T}.F_x.\mathbf{N}'.d\bar{x} \tag{19}$$

$$\mathbf{K} = \int_0^l \mathbf{N}''^\mathbf{T}.EI(\bar{x}).\mathbf{N}''.d\bar{x} \tag{20}$$

Where $\mathbf{M},\mathbf{K_G}$ and $\mathbf{K}$ are respectively consistent mass, geometric stiffness and flexural stiffness matrices. ρ and A are respectively mass per unit volume and cross-sectional area. F_x is the axial force i.e. centrifugal force which is given by

$$F_x = \Omega^2 \int_x^L x\rho A(x)dx \tag{21}$$

where Ω and L are respectively the rotational speed and whole length of the beam.

4. Numerical Examples and Discussion

The proposed method is employed to determine the natural frequencies of a beam whose cross-sectional area and moment of inertia vary respectively as,

$$A(x) = A_0\left(1 - c\frac{x}{L}\right) \quad I(x) = I_0\left(1 - c\frac{x}{L}\right)^3 \tag{22}$$

Where A0 and I0 are respectively cross-sectional area and moment of inertia at the origin and c is the taper ratio. The following dimensionless parameters namely rotational speed parameter η and dimensionless natural frequency μ are introduced to make comparisons with the literature.

$$\eta^2 = \frac{\rho A_0 L^4 \Omega^2}{EI_0} \quad \mu^2 = \frac{\rho A_0 L^4 \omega^2}{EI_0} \tag{23}$$

The effect of rotational speed parameter on the variation of natural frequencies for a tapered beam with taper ratio c = 0.5 is tabulated in Table 2. As expected, the natural frequencies increase with the rotational speed due to the stiffening effect of centrifugal force.

In Table 3, the natural frequencies are given for different values of taper ratio. The natural frequencies except for the first mode decrease with the taper ratio due to the softening effect caused by the decrease in cross-sectional area and moment of inertia.

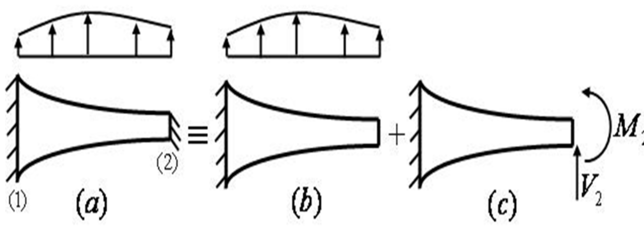

Figure 3.Decomposing the beam into two isostatic systems

Table 2 Effect of rotational speed on variation of dimensionless natural frequencies

η	Taper Ratio=0.5									
	First Mode		Second Mode		Third Mode		Fourth Mode		Fifth Mode	
	Present	Ref. [7]	Present	Ref. [7]	Present	Ref. [7]	Present	Ref. [7]	Present	Ref. [7]
0	3.8216	3.82379	18.3073	18.3173	47.25	47.2648	90.4873	90.4505	148.294	148.002
1	3.9845	3.98661	18.464	18.474	47.4024	47.4173	90.6407	90.6039	148.448	148.156
2	4.4347	4.4368	18.9267	18.9366	47.8567	47.8717	91.099	91.0625	148.91	148.619
3	5.0906	5.09267	19.6741	19.6839	48.6041	48.619	91.8574	91.8216	149.675	149.386
4	5.8767	5.87877	20.6754	20.6851	49.6306	49.6456	92.908	92.873	150.74	150.454
5	6.7412	6.7434	21.8957	21.9053	50.9187	50.9338	94.2405	94.2064	152.098	151.814
6	7.6529	7.65514	23.2997	23.3093	52.4481	52.4632	95.8421	95.809	153.739	153.46
7	8.5932	8.59557	24.8552	23.3093	54.1972	54.2124	97.6986	97.6666	155.656	155.38
8	9.5514	9.55396	26.5342	24.8647	56.1442	56.1595	99.7945	99.7638	157.835	157.564
9	10.5212	10.5239	28.3132	28.3227	58.268	58.2833	102.114	102.084	160.267	160.001
10	11.4988	11.5015	30.1733	30.1827	60.5486	60.5639	104.64	104.612	162.939	162.677

Table 3 Effect of taper ratio on variation of dimensionless natural frequencies

Taper Ratio	η=5					
	First Mode		Second Mode		Third Mode	
	Present	Ref. [7]	Present	Ref. [7]	Present	Ref. [7]
0.1	6.4891	6.49115	24.7685	24.7805	62.4880	62.5113
0.2	6.5370	6.53913	24.0847	24.0961	59.7289	59.7504
0.3	6.5931	6.59525	23.3797	23.3906	56.8916	56.9112
0.4	6.6599	6.66206	22.6510	22.6612	53.9615	53.9789
0.5	6.7412	6.7434	21.8957	21.9053	50.9187	50.9338
0.6	6.8432	6.84537	21.1118	21.1207	47.7356	47.7478
0.7	6.9762	6.97848	20.3004	20.3086	44.3720	44.3805
0.8	7.1604	7.16281	19.4777	19.4848	40.7701	40.7725
0.9	7.4411	7.44359	18.7364	18.7412	36.8803	36.8667

5. Conclusions

New shape functions are proposed for the analysis of rotating tapered beams which are obtained in terms of special structural functions namely BDFs. The superiority of the present method lies in proposing a mechanical solution rather than a mathematical one. The structural essence of BDFs let us obtain them using unit load method. Although BDFs are obtained on the basis of static deformations, it is observed that the method could be used in free vibration analysis and acceptable results could be expected even with a coarse mesh.

6. References

[1] R. H. Gallagher and C. H. Lee. Matrix dynamic and instability analysis with non-uniform elements. *Int J Numer Meth Eng 2* ,265-275,1970.

[2] D. L. Karabalis and D. E. Beskos. Static, dynamic and stability analysis of structures composed of tapered beams. *Comput Struct* 16, 731-748, 1983.

[3] J. R. Banerjee and F. W. Williams. Exact Bernoulli-Euler dynamic stiffness matrix for a range of tapered beam. *Int J Numer Meth Eng* 21, 2289-2302, 1985.

[4] M. Eisenberger. Exact solution for general variable cross-section members. *Comput Struct* 41, 765-772, 1991.

[5] J. R. Banerjee. Free vibration of centrifugally stiffened uniform and tapered beams using the dynamic stiffness method. *J. Sound Vibr*, 233(5), 857–75, 2000.

[6] J. R. Banerjee. Dynamics stiffness formulation and free vibration analysis of centrifugally stiffened Timoshenko beams. *J. Sound Vibr*, 247(1), 97–115, 2001

[7] J. R. Banerjee, H. Su, D.R. Jackson. Free vibration of rotating tapered beams using the dynamic stiffness method. *J. Sound Vibr*, 298, 1034-1054, 2006

[8] D. J. Hodges and M.J. Rutkowski. Free vibration analysis of rotating beams by a variable order finite element method. *AIAA J*, 19(11), 1459–66, 1981.

[9] K. M. Udupa, T.K. Varadan. Hierarchical finite element method for rotating beams. *J. Sound Vibr*, 138(3), 447- 56, 1990.

[10] A. D. Wright, G.E. Smith, R.W. Thresher and J.C.L. Wang. Vibration modes of centrifugally stiffened beams. *J Appl Mech*, 49, 197-202, 1982

[11] G. Wang, N.M. Wereley. Free vibration analysis of rotating blades with uniform tapers. *AIAA J* , 42 (12), 2429-2437, 2004.

[12] J. Babu Gunda and R. Ganguli. New rational interpolation functions for finite element analysis of rotating beams. *Int Jnl of Mech Sci*, 50, 578-588, 2008

[13] O. Ozdemir and M.O. Kaya. Flapwise bending vibration analysis of rotating tapered cantilever Euler-Bernoulli beam by differential transform method. *J Sound Vibr*, 289, 413-420, 2006.

[14] C. Mei. Application of differential transformation technique to free vibration analysis of a centrifugally stiffened beam. *Comput Struct* 86, 1280-1284, 2008.

[15] R. Attarnejad. On the derivation of the geometric stiffness and consistent mass matrices for non-prismatic Euler-Bernoulli beam elements. *Proceedings of European Congress on Computational Methods in Applied Sciences and Engineering*, Barcelona, 2000.

[16] R. Attarnejad. Free Vibration of Non-Prismatic Beams. *Proceedings of 15th ASCE Engineering Mechanics Conference*, New York, 2002.

[17] F. Arbabi. *Structural Analysis and Behavior*. McGraw-Hill Book, Inc., 1991.